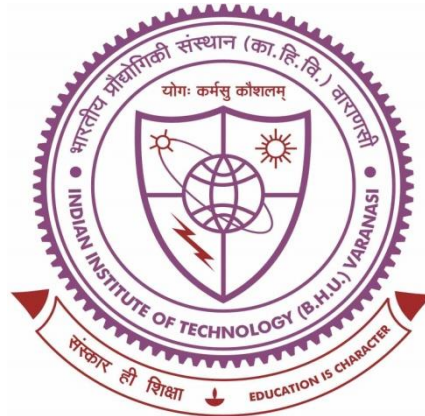


Fabrication and Characterization of Nanofibrous Scaffolds for Corneal Tissue Engineering Applications



**Thesis submitted in partial fulfillment
for the Award of Degree**

Doctor of Philosophy

by

Ajay Kumar Sahi

**SCHOOL OF BIOMEDICAL ENGINEERING
INDIAN INSTITUTE OF TECHNOLOGY (BHU)
(BANARAS HINDU UNIVERSITY)
VARANASI – 221005, (U.P.), INDIA**

CERTIFICATE

This is to certify that the revised thesis entitled "Fabrication and Characterization of Nanofibrous Scaffolds for Corneal Tissue Engineering Applications" is being submitted by Mr./Ms/Mrs Ajay Kumar Sahi in partial fulfilment for the award of Ph.D. in Department/School of Biomedical Engineering IIT (BHU), Varanasi is a record of bonafide work carried out by him/her.

Date of Submission: 16.03.2022

Sanjeev Kumar Mahto

Dr. Sanjeev Kumar Mahto
(Supervisor)
Associate Professor,
School of Biomedical Engineering,
Indian Institute of Technology (BHU),
Varanasi - 221005, (U.P.), India

(Co-supervisor)
(If any)

SUPERVISOR

Forwarded by:

Sanjeev Kumar Mahto

HoD/CoS
(Signature with Seal)
समन्वयक/CO-ORDINATOR
जैव चिकित्सा अभियांत्रिकी स्कूल
SCHOOL OF BIOMEDICAL ENGG.
भारतीय प्रौद्योगिकी संस्थान (का.हि.वि.)
INDIAN INSTITUTE OF TECHNOLOGY (B.H.U.)
वाराणसी-221005/VARANASI-221005

CERTIFICATE

It is certified that the work contained in the thesis titled “**Fabrication and Characterization of Nanofibrous Scaffolds for Corneal Tissue Engineering Applications**” by “**Ajay Kumar Sahi**” has been carried out under my supervision and this work has not been submitted elsewhere for a degree.

It is further certified that the student has fulfilled all the requirements of Comprehensive Examination, Candidacy and SOTA for the award of Ph.D. Degree.



(Dr. Sanjeev Kumar Mahto)
Supervisor
Associate Professor,
School of Biomedical Engineering,
Indian Institute of Technology (BHU),
Varanasi - 221005, (U.P.), India

सह-आचार्य/ASSOCIATE PROFESSOR
जैव चिकित्सा अभियांत्रिकी स्कूल
SCHOOL OF BIOMEDICAL ENGG
भारतीय प्रौद्योगिकी संस्थान (एच.ए.ए.)
INDIAN INSTITUTE OF TECHNOLOGY (B.H.U.)
वाराणसी-221005/VARANASI-221005

DECLARATION BY THE CANDIDATE

I, Ajay Kumar Sahi, am certified that the work embodied in this Ph.D. thesis is my own bonafide work and carried out by me under the supervision of Dr. Sanjeev Kumar Mahto from **21st July 2015 to 22nd July 2021** at the School of Biomedical Engineering, Indian Institute of Technology (BHU), Varanasi. The matter embodied in this thesis has not been submitted for the award of any other degree/diploma.

I declare that I have faithfully acknowledged and given credits to the research workers wherever their work has been cited in my work in this thesis. I further declare that I have not wilfully copied any other's work, paragraphs, text, data, results, etc., reported in journals, books, magazines, reports dissertations, theses, etc., or available at websites and have not included them in this thesis and have not cited as my own work.

Date: 22/07/2021

Place: Varanasi

**Signature of the Student
(Ajay Kumar Sahi)**

CERTIFICATE BY THE SUPERVISOR

It is certified that the above statement made by the student is correct to the best of our knowledge.

**(Dr. Sanjeev Kumar Mahto)
Supervisor**

Associate Professor,
School of Biomedical Engineering,
Indian Institute of Technology (BHU),
Varanasi - 221005, (U.P.), India

**(Prof. Prasun Kumar Roy)
Coordinator**

Professor
School of Biomedical Engineering,
Indian Institute of Technology (BHU),
Varanasi - 221005, (U.P.), India

सह-आचार्य/ASSOCIATE PROFESSOR
जैव चिकित्सा अभियांत्रिकी स्कूल
SCHOOL OF BIOMEDICAL ENGG
भारतीय प्रौद्योगिकी संस्थान (का.हि.वि.)
INDIAN INSTITUTE OF TECHNOLOGY (B.H.U.)
वाराणसी-221005/VARANASI-221005

समन्वयक/CO-ORDINATOR
जैव चिकित्सा अभियांत्रिकी स्कूल
SCHOOL OF BIOMEDICAL ENGG.
भारतीय प्रौद्योगिकी संस्थान (का.हि.वि.)
INDIAN INSTITUTE OF TECHNOLOGY (B.H.U.)
वाराणसी-221005/VARANASI-221005

COPYRIGHT TRANSFER CERTIFICATE

Title of the Thesis: Fabrication and Characterization of Nanofibrous Scaffolds
for Corneal Tissue Engineering Applications.

Name of the Student: Ajay Kumar Sahi

Copyright Transfer

The undersigned hereby assigns to the Indian Institute of Technology (BHU), Varanasi all rights under copyright that may exist in and for the above thesis submitted for the award of the Doctor of Philosophy.

Date: 22/07/2021

Place: Varanasi



Signature of the Student
(Ajay Kumar Sahi)

Note: However, the author may reproduce or authorize others to reproduce material extracted verbatim from the thesis or derivative of the thesis for author's personal use provided that the source and the Institute's copyright notice are indicated.

***Dedicated
To
My Beloved Parents,
My Loving Brothers
and Sister***

Table of Contents	Page No.
List of figures	xii
List of tables	xx
List of abbreviations	xxi
Preface	xxiv
Chapter 1	
Introduction.....	01
1.1 Cornea.....	02
1.1.1 Anatomy, Function and Composition of Cornea	02
1.1.2 Microstructure of Cornea	03
1.1.3 Functions of corneal layers	03
1.1.3.1 Corneal Epithelium.....	03
1.1.3.2 Bowman’s Layer	04
1.1.3.3 Stroma Layer.....	04
1.1.3.4 Descemet’s Membrane.....	05
1.1.3.5 Endothelium Layer	05
1.2 Problem and Needs	05
1.2.1 Corneal diseases and dystrophies.....	05
1.2.2 Burden of corneal diseases	06
1.3 Solutions for Health Issues Associated With the Cornea	07
1.4 Tissue Engineering.....	08
1.4.1 Definition of Tissue Engineering	08
1.4.2 Cell sources in Tissue Engineering.....	09
1.4.3 Biomaterials in Tissue Engineering.....	10
1.4.4 Tissue Engineering Scaffolds	11
1.4.4.1 Hydrogel based scaffolds.....	13
1.4.4.2 Electrospinning nanofibrous scaffolds.....	13
1.4.4.3 Gas foaming.....	16
1.4.4.4 Solvent casting/Particulate leaching.....	17
1.4.4.5 Three-dimensional (3D) Bioprinting/Freeform fabrication technology ..	18
1.4.4.6 Decellularization technology	20
1.5 Literature review	23

1.6 Research objectives	25
1.7 Thesis outline	26
1.8 References	28
Chapter 2	
Fabrication, Characterization and Modification Strategy of Electrospun Nanofibrous Scaffolds from Acid and Alkaline Hydrolyzed Gelatin for Corneal Tissue Engineering	43
2.1 Introduction	44
2.2 Materials and method	50
2.2.1 Materials	50
2.2.2 Methods	50
2.2.2.1 Fabrication of electrospun gelatin nanofibrous mats	50
2.2.2.2 Preparation of Silk Fibroin Solution	52
2.2.2.3 Silk permeation inside gelatin scaffold	53
2.2.3 Characterization of the scaffolds	54
2.2.3.1 Morphological characterization of electrospun nanofibers	54
2.2.3.2 Porosity determination	55
2.2.3.3 ATR-FTIR spectroscopic analysis	55
2.2.3.4 Water retention capacity	56
2.2.3.5 In vitro stability and degradation	56
2.2.3.6 Transparency determination	57
2.2.3.7 Cellular viability and compatibility	57
2.2.3.7.1 Culturing fibroblast cells on the prepared nanofibrous scaffolds	57
2.2.3.7.2 MTT assay	58
2.2.3.8 Statistical analysis	59
2.3 Results	59
2.3.1 Morphological characterization	59
2.3.2 Posrosity determination	61
2.3.3 ATR-FTIR spectroscopic analysis	62
2.3.4 Liquid retaining capacity	66
2.3.5 Stability and degradation	68
2.3.6 Transparency	69
2.3.7 Cellular viability and compatibility	71

2.3.7.1 Cell culture within the scaffolds	71
2.3.7.2 MTT assay	73
2.4 Discussion.....	74
2.5 Conclusion	79
2.6 References	81
Chapter 3	
Fabrication and Characterization of Silk Fibroin Based Nanofibrous Scaffolds Supplemented with Gelatin for Corneal Tissue Engineering	
96	
3.1 Introduction.....	97
3.2. Materials and method.....	101
3.2.1 Materials	101
3.2.2 Methods.....	102
3.2.2.1 Preparation of Silk Fibroin Solution.....	102
3.2.2.2 Fabrication of electrospun nanofibrous mats.....	102
3.2.2.3 Permeation of gelatin solution inside electrospun silk scaffold ..	104
3.2.3 Characterization of the scaffolds.....	104
3.2.3.1 Morphological characterization of electrospun nanofibers	104
3.2.3.2 Porosity determination	105
3.2.3.3 ATR-FTIR analysis.....	105
3.2.3.4 Liquid retention capacity	106
3.2.3.5 In vitro stability and degradation.....	106
3.2.3.6 Transparency determination	106
3.2.3.7 Water contact angle measurement	107
3.2.3.8 Mechanical testing of the Scaffold.....	107
3.2.4 Cellular viability and compatibility	108
3.2.4.1 Culturing of cells within scaffolds	108
3.2.4.2 Nuclear staining	109
3.2.4.3 MTT assay	109
3.2.5 Statistical Analysis	110
3.3 Results	111
3.3.1 Characterization of the scaffolds.....	111
3.3.1.1 Morphological characterization of electrospun nanofibers	111
3.3.1.2 Porosity determination	113

3.3.1.3 ATR-FTIR spectroscopic analysis.....	114
3.3.1.4 Liquid retention capacity	116
3.3.1.5 Stability and degradation of electrospun nanofibers.....	117
3.3.1.6 Transparency measurement	120
3.3.1.7 Contact angle measurement	122
3.3.1.8 Mechanical testing of the scaffolds.....	123
3.3.1.9 Cell compatibility	124
3.3.1.10 MTT Assay	126
3.4 Discussion.....	127
3.5 Conclusion	137
3.6 References.....	138
Chapter 4	
Conclusion and future scope of work.....	150
Permission from Central Animal Ethical Committee	157
List of publications	162

LIST OF FIGURES

Figure No.	Figure description	Page No.
Figure 1.1	Diagram and anatomy of human eye.	02
Figure 1.2	Diagram showing microstructure of cornea and its function	03
Figure 1.3	(A) Global map of age-standardized prevalence of blindness, 1990-2020. Source: Vision Atlas (B) represents the requirement and availability of healthy donor cornea.	06
Figure 1.4	General Scheme of Tissue Engineering Process.	08
Figure 1.5	A diagrammatic representation of the difference between a two-dimensional and three-dimensional cell culture environment.	12
Figure 1.6	Approaches for developing a wide range of 3D scaffolds.	12
Figure 1.7	Diagrammatic representation of electrospinning unit setup and Taylor cone formation.	14
Figure 1.8	Depicts various applications of electrospun nanofibers.	15
Figure 1.9	Schematic diagram for fabrication of hierarchical scaffolds with a tailored macro porous (3D printing) /micro-porous (gas foaming) architectures.	17
Figure 1.10	Schematic diagram for fabrication of scaffolds using solvent casting/ salt leaching method	18
Figure 1.11	Overview of 3D Bioprinting for Tissue Engineering. Computer aided design models use patient derived images to mimic the specific geometry of tissues of interest. The printing bioink may contain a combination of biomaterials, bioactive molecules, or cells to create functionalized and personalized scaffolds. Scaffolds are then printed using the computer aided design and desired bioink (s).	19
Figure 1.12	Schematic of organ decellularization and tissue decellularization approaches.	22

Figure 1.13	Schematic diagram displaying applications of decellularized materials.	23
Figure 2.1	Basic chemical structure of gelatin.	44
Figure 2.2	Basic amino acid composition of gelatin.	45
Figure 2.3	Preparation of two distinct gelatins from collagen hydrolysis by acidic and basic treatments	46
Figure 2.4	Depicts schematic for electrospinning setup and optimized parameters for gelatin electrospinning	51
Figure 2.5	Schematic flow diagram for silk fibroin extraction procedure.	52
Figure 2.6	Schematic procedure for (A) silk permeation inside the electrospun gelatin A nanofibrous structure and (B) schematic representing ethanol vapor crosslinking of the silk permeated gelatin A nanofibrous (SFG) scaffold. Ethanol vapor treatment alters silk confirmation from least stable, high water soluble scaffold to highly stable, less water-soluble silk. Therefore, the gelatin nanofibers of silk permeated gelatin A (SFG) remains protected from fast degradation enhancing its stability under physiological conditions.	54
Figure 2.7	Schematic for porosity analysis using Image J software.	55
Figure 2.8	Depicts the mechanism of MTT assay to determine the cellular proliferation.	59
Figure 2.9	Digital images and SEM micrograph of the electrospun gelatin nanofibers. (A) Digital images and (B) SEM images of nanofibrous scaffold shows no difference except gelatin B nanofibers appears smooth and thin compared to gelatin type A nanofibers.	60
Figure 2.10	Depicts digital images of electrospun gelatin A (GA) silk	61

permeated nanofibrous gelatin A (SFG), and their respective SEM images.

Figure 2.11 Graph represents the porosity percentage obtained using image J software from the scanning electron microscope (SEM) images of the fabricated scaffolds: gelatin A and gelatin B. 62

Figure 2.12 Attenuated total Reflection-Fourier-transform infrared spectroscopy (ATR-FTIR) analysis of electrospun gelatin A scaffold, gelatin B scaffold. Both the gelatin A and B polymeric scaffolds show similar characteristic peaks with no significant difference. Gelatin A and gelatin B scaffolds represents characteristic peaks at 1640, 1540, 1455 cm^{-1} and 3304 cm^{-1} for amide I, amide II, amide III and amide A, respectively. 64

Figure 2.13 Attenuated total reflection-Fourier-transform infrared spectroscopy (ATR-FTIR) analysis of electrospun gelatin A scaffold silk film, and ethanol treated silk permeated gelatin A nanofibrous mat [SFG (T)]. SFG (T) shows all the characteristic peaks of gelatin A and silk, with a peak shift of silk characteristic peak to a slightly lower wavenumber, i.e., at 1627 cm^{-1} , 1522 cm^{-1} , and 1232 cm^{-1} for amide I, amide II, and amide III, respectively. 65

Figure 2.14 Water retention percentage of acid hydrolyzed (gelatin A) scaffold at (A) room temperature (B) at 37°C (physiological temperature) upto 11 h, and (C) electrospun silk permeated gelatin A nanofibrous (SFG) scaffold at 37°C (physiological temperature) up to 144 h (i.e. 6 days). The gelatin A scaffold incubated at 37°C shows high water holding capacity, but starts degrading after 5 h whereas the samples stored at a room temperature (25°C) remains stable upto 11 h of incubation. Silk permeated electrospun gelatin 67

A nanofibrous scaffold (SFG) remain stable for longer compared to gelatin A alone, providing better opportunity for cellular growth.

Figure 2.15 Depicts in vitro degradation of scaffolds in lysozyme solution to simulate the in vivo environment of body fluids (A) Digital images of scaffolds showing physical appearance of gelatin A, gelatin B and SFG scaffolds after 4h, 10h, 1 day, 3 day and 6 days of incubation in lysozyme solution (B) Represents weight loss percentage of scaffolds after 4 h, 10 h, 1 day, 3 day and 6 days of incubation. Scale bar is 10 mm. 69

Figure 2.16 Depicts the transparency percentage of the native rat cornea and fabricated electrospun gelatin type A scaffold and silk permeated gelatin A (SFG) nanofibrous scaffolds. The scaffolds illustrates comparable transparency with respect to native adult rat cornea. 70

Figure 2.17 Illustrates growth of SIRC [Statens Seruminstitut Rabbit Cornea] fibroblast cells cultured on (A) a culture plate and (B) silk permeated gelatin A (SFG) nanofibrous scaffold for 1, 3, and 5 days. Scale bar is 100 μ m. 72

Figure 2.18 This figure illustrates the percentage cellular viability of SIRC [Statens Seruminstitut Rabbit Cornea] fibroblast cells for 1st, 3rd and 5th day of cell culture. Cellular proliferation and compatibility of the electrospun gelatin A permeated nanofibrous (SFG) scaffold determined by MTT assay. In this experiment, absorbance for the 5th day control culture of SIRC cell was considered as reference OD for all the samples. Values are expressed as mean \pm SD (n=3) and the level of significance as *p < 0.05 and **p < 0.01, ***p < 0.001, respectively. 73-74

	Morphological analysis through SEM photomicrographs of SF (in aqueous), SF (in formic acid) and gelatin-permeated SF (in formic acid). Scaffolds along with their respective digital images (a)	
Figure 3.1	before ethanol vapor treatment i.e., SF (in aqueous; NT), SF (in formic acid; NT), gelatin-permeated SF (in formic acid; NT) and (b) after ethanol vapor treatment i.e., SF (in aqueous; T), SF (in formic acid; T), gelatin-permeated SF (in formic acid; T).	112
Figure 3.2	Representative image shows continuous gelatin permeation throughout the internal space of the silk nanofibrous scaffold gelatin-permeated SF (in formic acid) without leaving any air space along with negligible or no sign of any bubble entrapment within the nanofibrous structure. Scaffolds were cut across the longitudinal plane to observe the extent of gelatin permeation through the SEM.	113
Figure 3.3	Diameter distribution of nanofibers of electrospun SF (in formic acid; NT) scaffolds along with its nanofiber orientation graph.	114
Figure 3.4	ATR-FTIR spectra of SF (in aqueous; NT), SF (in formic acid; NT), gelatin-permeated SF (in formic acid; NT), SF (in aqueous; T), SF (in formic acid; T) and gelatin-permeated SF (in formic acid; T). (Where NT= non-treated, T= ethanol treated).	115
Figure 3.5	Graph shows weight gain percentage of ethanol treated samples namely, gelatin-permeated SF (in formic acid; T), SF (in formic acid; T), SF (in aqueous; T) and non-treated samples namely, gelatin-permeated SF (in formic acid; NT), SF (in formic acid; NT) and SF (in aqueous; NT).	117
Figure 3.6	Depicts (a) digital images representing stability of prepared	118

nanofibrous scaffolds in PBS at a room temperature (b) digital images of scaffolds held through forceps after 14 days immersed in PBS at 37°C, (c) digital and SEM micrographs of electrospun samples after 14 days degradation in a lysozyme containing solution at 37°C (d) graph shows weight loss percentage of samples over 14 days of immersion in a lysozyme containing solution at 37°C. (Where NT= non-treated, T= ethanol treated).

Figure 3.7

Transparency of different scaffolds namely SF (in aqueous), SF (in formic acid), gelatin-permeated SF (in formic acid) before (NT) and after ethanol vapor treatment (T) in PBS at a room temperature (25°C) (a) digital images of samples showing visual transparency (b) shows the physical appearance of ethanol treated scaffolds in PBS and (c) graph shows percentage of light transmission through the samples. Scale bar: 10 mm. (where NT= non-treated, T= ethanol treated).

121

Figure 3.8

Represents the contact angles of non-treated SF (in aqueous; NT), SF (in formic acid; NT) and gelatin-permeated SF (in formic acid; NT) and their ethanol treated forms namely, SF (in aqueous; T), SF (in formic acid; T) and gelatin-permeated SF (in formic acid; T) indicating the wetting behaviour of scaffolds. (where NT= non-treated, T= ethanol treated)

122

Figure 3.9

Depicts the tensile stress-strain curve of non-treated SF (in aqueous; NT), SF (in formic acid; NT) and gelatin-permeated SF (in formic acid; NT) and their ethanol treated forms namely, SF (in aqueous; T), SF (in formic acid; T) and gelatin-permeated SF (in formic acid; T) indicating the mechanical stability of respective scaffolds. (Where NT= non-treated, T= ethanol treated).

124

The above panel of images represents the cells cultured within the ethanol treated SF (in aqueous; T) scaffold using (a) corneal fibroblast SIRC cells (DAPI staining) and (b) L929-RFP fibroblast cells for over a period of 6 days. (c) Represents SIRC cells (DAPI staining) cultured on gelatin-permeated SF (in formic acid; T) and (d) L929-RFP cells cultured on gelatin-permeated SF (in formic acid; T) scaffolds for over a period of 6 days. Scale bar is 100 μ m for bright field, fluorescent and merged images. (Where NT= non-treated, T= ethanol treated).

Figure 3.10 125

The figure illustrates the percentage cellular viability of (a) SIRC cells (b) L929-RFP cells for 2, 4 and 6 days and the cytocompatibility of the scaffolds as determined by MTT assay (c) comparative cell proliferation percentage values of cells cultured on SF (in aqueous; T) and gelatin-permeated SF (in formic acid; T) scaffolds. In this experiment, absorbance for the 6th day culture of positive control was considered as reference OD for all the samples. Values are expressed as mean \pm SD ($n = 3$) and the level of significance as $***p < 0.05$. (Where NT= non-treated, T= ethanol treated)

Figure 3.11 127

Represents (a) digital images of gelatin-permeated SF (in formic acid) and silk-gelatin blend (SF/G blend (in formic acid)) placed in PBS showing visual transparency [scale bar = 10 mm] (b) Transparency of gelatin-permeated SF (in formic acid) composite and SF/G blend (in formic acid) scaffolds before (NT) and after ethanol vapor treatment (T) in PBS at a room temperature (25°C) and (c) Their comparative bar graph displaying low level of transparency for SF/G blend (in formic acid) compared to gelatin-

Figure 3.12 134

permeated SF (in formic acid) composite. (Where NT= non-treated, T= ethanol treated).

LIST OF TABLES

Table No.	Table description	Page No.
Table 2.1	Characteristics of gelatin type A and type B as described in the literatures.	47
Table 2.2	Transparency percentage of the fabricated scaffold quantified using UV-Visible spectrophotometer.	71
Table 3.1	List of a few-reported scaffolds promising for corneal tissue engineering and their relative properties against our fabricated product.	99-101
Table 3.2	Optimized values of electrospinning parameters for the prepared formulations.	103
Table 3.3	Weight loss percentage of scaffolds after 14 days of incubation of treated and non-treated samples.	119
Table 3.4	Transparency percentage of the fabricated scaffolds quantified using UV-Visible spectrophotometer.	121

LIST OF ABBREVIATIONS AND SYMBOLS

ECM	Extracellular matrix
WHO	World Health Organization
VLEG	Vision Loss Expert Group
IAPB	The International Agency for the Prevention of Blindness
PKP	Penetrating Keratoplasty
LK	Lamellar Keratoplasty
SFF	Solid Freeform Fabrication
mL/h	Millilitre per hour
µm	Micrometre
PGA	Poly(glycolic acid)
PLA	Poly(lactic acid)
PVA	Poly (vinyl alcohol)
PLGA	Poly (lactic acid-co-glycolic acid)
SNF	Silk Nanofibrils
GelMA	Gelatin Methacryloyl
EGCG	Epigallocatechin Gallate
PDMS	Polydimethylsiloxane
SDS	Sodium Dodecyl Sulfate
HS	Hypertonic Saline
ATPase	Adenosinetriphosphatase
NG	N ₂ gas
SLG	Sodium N-lauroyl glutamate
CAD	Computer-aided design
DNA	Deoxyribonucleic acid
dPC	Decellularized porcine corneal
HHP	High Hydrostatic Pressure
TCP	Tissue culture polystyrene
%	Percentage
PG	PicoGreen
kPa	Kilo Pascal
2D	Two-dimensional
3D	Three-dimensional

TFE	Trifluoroethanol
RGD	Arginine-Glycine-Aspartate
MWCO	Molecular weight cut off
FBS	Fetal Bovine Serum
DMEM	Dulbecco's modified Eagle's medium
GAA	Glacial Acetic Acid
SRL	Sisco Research Laboratories
PEG	Polyethylene glycol
nm	Nanometre
PLA	Polylactic acid
LiBr	Lithium bromide
EDC	1-Ethyl-3-(3-dimethylaminopropyl)-1-carbodiimide hydrochloride
NHS	N-Hydroxysuccinimide
SEM	Scanning electron microscopy
MTT	(3-(4,5-Dimethylthiazol-2-yl)-2,5-Diphenyltetrazolium Bromide)
SFG	Silk permeated gelatin A nanofibrous scaffold
SIRC	Statens Seruminstitut Rabbit Cornea
DMSO	Dimethyl Sulfoxide
ANOVA	Analysis of variance
mm	millimetre
mM	Milli molar
μ M	Micro molar
μ g	Microgram
CO ₂	Carbon dioxide
RT	Room temperature
μ L	Microlitre
rpm	Rotations per minute
DIV	Days in vitro
PBS	Phosphate buffer saline
BSA	Bovine serum albumin
DAPI	(4,6-diamidino-2-phenylindole)
PGA	Poyglycolic acid
PCL	Polycaprolactone

PVA	Polyvinyl alcohol
PH	Psyllium husk
G	Gelatin
ATR	Attenuated total reflection
FTIR	Fourier transform infrared
t	Time
TEBM	Tissue Engineering and Biomicrofluidics

The cornea is the eye's outermost layer and together with the eyelids and sclera protects the interior of the eye. The cornea accounts for 75% of the eye's refractive power and it is transmitting almost all visible light into the eye. It is a thin, elastic, non-vascularized tissue that adjusts the curvature of the eye and comprised of five separate layers and three distinct cell types. Bilateral corneal blindness affects over 10 million people globally. Corneal disease, second only to cataracts, is a leading cause of blindness. Currently, the only way to restore eyesight is via corneal transplantation. Total corneal transplantation has a 90% success probability in individuals with favorable prognoses (minimal graft vascularization and inflammation), but virtually no chance in patients with alkali burns or repeated graft failures. Among the disadvantages of corneal transplantation, include high rates of immunological rejection, the risk of infection and donor scarcity.

As a viable alternative to donated corneas, a tissue-engineered cornea stromal replacement may provide substantial advantages. Tissue engineering has emerged as a potentially wide field that may result in the creation of synthetic corneal stromal equivalent tissues. The approach faces several difficulties, including the following: (1) selecting the type of corneal cell and its isolation; (2) developing a suitable biomaterial scaffold that promotes cell growth and differentiation; and (3) replicating the intricate, sophisticated architecture of the tissue with uniformly aligned architecture, resulting in corneal tissue with optimal transparency, refractive power, and mechanical stability. (4) Recreating a non-vascularized and innervated environment that guarantees the tissue's survival by sustaining the tissue's high metabolic requirement while also maintaining transparency.

The enabling scaffold fabrication technologies for tissue engineering open new possibilities to mimic the native microenvironment of a cell suitable enough to contribute to the overall functions of a particular cell or tissue. In the present thesis, we have developed various functional three-dimensional micro- and nanoscale structures using electrospinning approach. Collagen biomaterials are the most suitable materials for fabricating corneal analogues because the vast majority of the corneal stroma is composed of various types of collagen organized in an intricate architecture. Due to the high expense of collagen, its hydrolysate gelatin may be utilized in lieu of the collagen to form an extracellular matrix. Due to the fact that gelatin may be hydrolyzed in two distinct ways, it is essential to utilize an appropriate form of gelatin while fabricating nanofibrous scaffolds. As a result, a comparative research is performed to identify which form of gelatin should be utilized in the construction of nanofibrous scaffolds. To the best of our current knowledge, there remains no reports concerning the study related to acid hydrolyzed gelatin (gelatin A) and alkaline hydrolyzed gelatin (gelatin B) nanofibrous scaffolds together. We have made an attempt to compare these gelatin based nanofibrous scaffolds that are constructed with the use of a ternary solvent (glacial acetic acid/ethyl acetate/water). Electrospinning methods provide gelatin scaffolds a high surface-to-volume ratio as well as a high porosity. The electrospun scaffold based on gelatin A has a water retention capacity of about 800% and is found very stable at ambient temperature. Similarly, its transparency is similar to that of adult rat cornea, making it a viable option for corneal tissue growth.

In addition, without crosslinking the gelatin A nanofibrous sheet is found incapable of enduring physiological circumstances on its own for longer duration. As a result, penetration of silk into the gelatin scaffold followed by physical crosslinking (with ethanol vapor) significantly increases its stability. The nanofibrous gelatin A scaffold

permeated with silk fibroin (SFG) provides optimal stability as well as proliferation for corneal fibroblast cells close to 72% compared to that of the 5th day control. Chemical or enzymatic cross linkers may be used to further adjust the degradation rate and stability depending on the application. Thus, the comparison results indicate that the SFG scaffold is more stable than gelatin A alone; enabling it potentially helpful in corneal tissue engineering application.

We also present the successful development of a new nanocomposite gelatin hydrogel system reinforced with mechanically robust silk nanofibers. The permeation of gelatin into the silk nanofibrous scaffold improved the proportion of visible light transmission, increasing its usefulness in a variety of applications where transparency is critical, such as skin wound dressing and most significantly ocular tissue constructions. Ethanol vapor treatment of silk nanofibers resulted in the change of the less stable random helical conformation to the more stable sheets shape. Scanning electron microscopy (SEM) micrographs were used to examine the micro/nano-scale characteristics of the constructed scaffolds. Fourier transform infrared spectroscopy (FTIR) showed characteristic peaks associated with polymeric functional groups and their changes after ethanol vapor treatment. The liquid retention capacity of gelatin-permeated SF (in formic acid; T) [T= Treated] was found to be significantly greater than that of SF (in aqueous; T) and SF (in formic acid; T). All scaffolds were shown to be substantially stable for up to 14 days when incubated in phosphate buffered saline (PBS) at 37°C, except the untreated SF (in aqueous; NT) [NT= Non-treated]. In comparison to untreated samples, treated samples demonstrated substantially improved physical and microscopic stability. The degradation analysis showed that all ethanol-treated samples exhibited improved and enhanced stability. The cytocompatibility of corneal fibroblast SIRC cells and L929-RFP fibroblast cells was shown to be much higher in the gelatin-permeated SF (in formic acid; T)

scaffold than in the other scaffolds. The novelty of this study is the creation of a nanofibrous silk-gelatin composite scaffold that exhibits superior transparency, mechanical strength and cellular biocompatibility. Overall, the results indicated that the addition of gelatin to nanofibrous silk scaffolds resulted in durable, highly cytocompatible and transparent scaffolds; making them an excellent option for corneal tissue engineering. Although the material was effectively characterised in vitro in the current research, further extensive in vivo characterization is needed to verify the suggested materials for creating corneal stromal equivalents. Electrospun gelatin and silk nanofibers have received little attention in the area of corneal tissue engineering for the purpose of recreating corneal equivalents, leaving space for future research.

To summarize, the present thesis demonstrates the development and fabrication of various three-dimensional microscale structures employing the enabling electrospinning technology.

Keywords:

Cornea, gelatin, silk fibroin, electrospinning, tissue engineering, scaffolds, extracellular matrix.